Grazer Schriften der Geographie und Raumforschung **Band 41 / 2006** pp. 37 - 48

Glacier Mapping in High Mountains Using DEMs, Landsat and ASTER Data

Tobias Bolch (1) and Ulrich Kamp (2)

(1) Dresden University of Technology, Germany
(2) The University of Montana, U.S.A.

Abstract

Glaciers are sensitive climate indicators and thus subject to monitoring of environmental and climate changes. Remote sensing techniques are often the only way to analyze glaciers in remote mountains and to monitor a large number of glaciers at the same time. Although several glacier mapping methods exist, often, results are still not good enough for in-depth conclusions. In particular, this is true for debris-covered glaciers. For the Bernina Group in the Swiss Alps and for the northern Tien Shan in Kazakhstan and Kyrgyzstan a glacier mapping was undertaken employing digital elevation models (DEMs). DEMs were generated from ASTER and SRTM3 data and compared with each other and -for the Bernina Group- compared with the Swiss DHM25L2. Whereas ASTER DEM elevations are too high on average, SRTM3 DEM elevations are slightly too low. However, both DEMs are of good use for glacier delineation. The glacier mapping approach includes Landsat TM4/TM5-ratio images, multispectral and morphometric analysis. Results are satisfying for debris-free and larger debris-covered glaciers in both study areas. The next step should be an automated glacier mapping method.

KEYWORDS: Glacier mapping, debris-covered glacier, DEM analysis, morphometric analysis, ASTER DEM, SRTM DEM, Tien Shan, Swiss Alps

1. Introduction

Mountain glaciers interact sensitively with climate and therefore they are climate indicators (Oerlemans, 1994). The international program Global Land Ice Measurements from Space (GLIMS) monitors extent, changes, and dynamics of glaciers worldwide using satellite data, particularly from the ASTER sensor (Bishop et al., 2004; Kargel et al., 2005). Much work has been done to analyze glaciers and glacier changes using remote sensing techniques (Bishop et al., 2000; Della Ventura et al., 1987). For instance, several methods such as supervised classification or thresholding of ratio images are available to delineate the glacier ice (Bayr et al., 1994; Gratton et al., 1990; Paul et al., 2002; Sidjak and Wheate, 1999). Thresholding of ratio images after a time-intensive manual digitizing was found to be the most accurate method (Paul, 2000). However, all such (semi-)automated methods failed to include debris-covered glacier areas due to spectral similarity to surrounding bedrock (Hempel, 2005). Consequently, debris-covered glaciers are still mapped mostly manually, which is time-intensive and therefore not suitable for studying larger areas (Paul, 2002; Williams et al., 1997). Recent mapping approaches focus on a more accurate mapping of debris-covered glaciers (Paul et al., 2004). The aim of this study is to show the capability of accurate glacier mapping using multispectral data, digital elevation models (DEMs), and morphometric analysis for the Bernina Group in the Swiss Alps and for the northern Tien Shan in Kazakhstan and Kyrgyzstan. For the entire Swiss Alps, an accurate DEM with 25 m horizontal resolution exists. However, for the Tien Shan and many other high mountain regions high quality DEMs are not available, but DEMs can be generated from ASTER or SRTM data.

2. Background and Previous Studies

Not only in the Himalayas, but also in the Alps and other high mountains like the Tien Shan many valley glaciers are partially covered by supraglacial debris. Glacier retreat often causes a relative increase in debris-covered glacier area. For instance, for the Tschierva Glacier in the Bernina Alps our own multitemporal remote sensing analysis of Landsat imagery show an increase of the glacier's debris-covered area by 1% between 1992 and 1999.

One way to distinguish between a debris-covered glacier and surrounding bedrock is by using surface temperatures as the supraglacial debris is often cooler due to the underlying ice. Ranzi et al. (2004) documented the high potential of using the thermal signature from ASTER and Landsat imagery for glacier mapping. Another approach to debris-covered glacier mapping is to include morphometric parameters such as slope and curvature. Models for morphometric classifications based on the hierarchical organization of topography where presented by Dikau et al. (1995). Bishop et al. (2001) presented a two-folded hierarchical model including elevation, slope, aspect and curvature derived from a SPOT DEM for debris-covered glaciers at Nanga Parbat in Pakistan. Paul et al. (2004) followed a semi-automated approach mapping a debris-covered glacier in the Swiss Alps from a TM4/TM5-ratio image and using the slope (<24°). Further improvements of the glacier map were then reached from a vegetation classification using multispectral data, neighborhood analyses and change detection. This approach required a DEM of high accuracy such as the Swiss DHM25L2 with 25 m horizontal resolution (Swisstopo 2004).

However, such detailed DEMs are not available for many other mountain areas. ASTER data allow for the generation of DEMs with a horizontal resolution of 30 m, and in addition multitemporal data sets allow for comparisons of DEMs from one location. Although in high mountains the extreme topography makes the DEM generation in general more difficult, ASTER DEMs can still be of good accuracy and useful for geomorphologic and glacier mapping (Bolch and Kamp, 2003; Eckert et al., 2005, Gspurning and Sulzer, 2004; Kääb et al., 2003; Kamp et al., 2005, Paul et al., 2004). Accurate ASTER DEMs require precise ground control points (GCPs), which should be well-distributed over the scene and different altitudes (Bolch et al., 2005; Eckert et al., 2005). Unfortunately, for many remote mountains exact GPS measurements of GCPs often require intense and difficult field campaigns. Artifacts might be introduced to the DEM, if the ASTER scene is not nearly cloud-free (<5 – 10% clouds). However, artifacts in the ASTER DEM can be substituted by SRTM3 data of 90 m horizontal resolution (Bolch et al., 2005). Although even DEMs from SRTM3 data show artifacts in extreme topographies, they can still be of similar or even higher accuracy than ASTER DEMs (Büyüksalih et al., 2004; Jacobsen 2005). SRTM3 data can easily be downloaded for free from the internet.

3. Study Areas

The first study area includes the Bernina Group in the Central Alps at the border between Switzerland and Italy (Figure 1a). The highest peak Piz Bernina (46°22'N, 9°54'E) is at 4049 m asl. The Bernina Group is one of the heaviest glaciated areas in the European Alps. Its glaciers are mostly mountain glaciers, but several valley glaciers exist reaching down to 2100 m asl. Larger glaciers are often partly covered with debris.

The second study area includes Zailiskiy and Kungey Alatau (42°30'– 43°30'N; 75°–79°E) in the northern Tien Shan of Kazakhstan and Kyrgyzstan (Figure 1b). From the Kazakh Steppe at 800 m asl. to the north both mountain

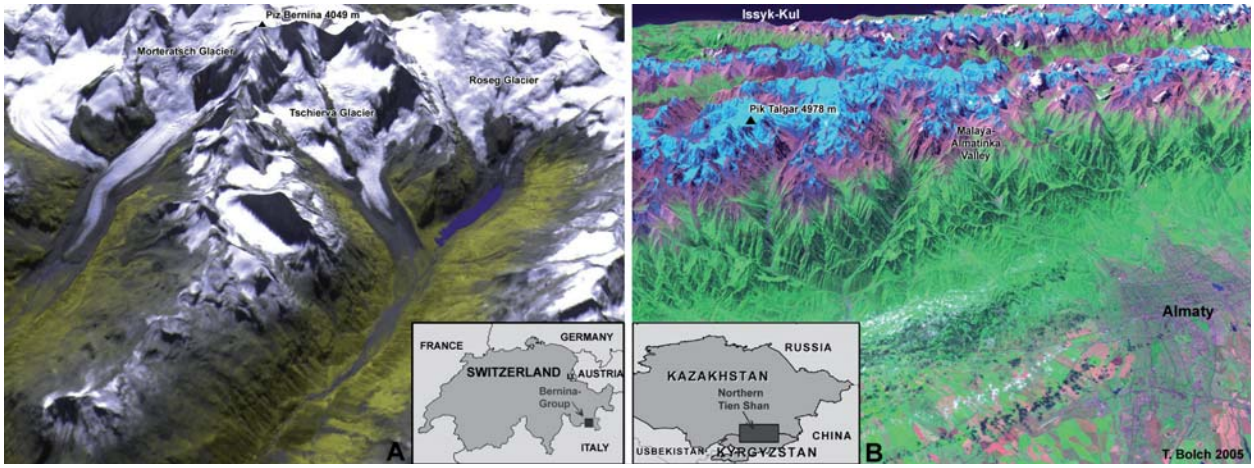

Figure 1: Source: DHM25 (©Swisstopo), ASTER-Scene from Oct. 2004 (Layers 3-3-1); B: Northern Tien Shan, Source: SRTM3-DEM, Landsat-scene from Aug. 1999 (Layers: 7-4-2); DHM25 reproduced with the permission of swisstopo (BA057533).

ranges rise up to nearly 5000 m asl. Lake Issyk-Kul at 1608 m asl. lies to the south. Although a general continental climate, great climatic differences can occur over small distances. Mostly mountain glaciers and several valley glaciers do exist reaching down to 3500 m asl. Whereas most of the glaciers are nearly debris-free, larger glaciers are partly covered with debris.

4. DEM Generation

4.1. Bernina Group, Swiss Alps

For the Bernina Group in the Swiss Alps a precise DEM of 25 m horizontal resolution is available (Swisstopo 2004). The level two-product (DHM25L2) includes improved topological information such as surfaces of glaciers and moraines. It represents the topography and glacier extents in 1991. For the ASTER Level 1A data from September 17, 2004 many clouds cover the southern part of the scene, whereas the northern slopes and most parts of the southern slopes of the Bernina Group are cloud-free. The ASTER DEM was generated using PCI Geomatica OrthoEngine 8.2. The generation included 25 GCPs (based on field measurements and the Topographic Map of Switzerland 1:25,000) and 51 tie points (TPs) from different altitudes, and the preliminary DEM was then recalculated with the highest level of detail. The RMSEx,y was <15 m for the GCPs and 4 m for the TPs. The resulting DEM still contained many artifacts like non-existing holes on steep slopes and non-existing peaks and pits especially under clouds, in ice-covered areas and in water bodies. For DEM improvement, the holes where interpolated automatically using a spline algorithm. To eliminate the peaks and pits and for smoothing reasons contour lines were calculated from the DEM, then manually improved and finally interpolated with the spline-with- tension algorithm. Although the overall quality of the final ASTER DEM is satisfactory, it is of lower quality than the Swiss DHM25L2. The overall quality of the SRTM3 DEM for this study area is good, although data holes exist along the entire ridge around the highest peak, particularly at the southern slopes. Since the holes were too large for an automated interpolation, they were filled with ASTER DEM data using the software SAGA.

Both ASTER and SRTM3 DEMs were compared with the DHM25L2. The elevations in the ASTER DEM are often too high, strictly speaking 8.3 m on average (Figure 2, Table 1). A high RSMEz of 28.4 m and a high standard deviation of 43.7 m might contribute to such inaccuracies. Although the maximum deviation of +330 m and the minimum deviation of -269 m are also very high, this is not unusual for high mountains (Kääb et al., 2003). Highest deviations can be found at steep slopes. In contrast to this, the elevations in the SRTM3 DEM are often too low, namely -9.8 m on average (Figure 2, Table 1). In general, it appears much smoother than the ASTER DEM. The maximum deviation of +210 m occurs, again, at steep slopes. The lower horizontal resolution of the SRTM3 DEM and a smoother topography might attribute to inaccuracies. For instance, small gullies and lateral moraines are difficult to identify. However, despite all inaccuracies both ASTER DEM and SRTM3 DEM can be used for mapping glacier extents.

4.2. Northern Tien Shan, Kazakhstan and Kyrgyzstan

For the northern Tien Shan in Kazakhstan and Kyrgyzstan no DEM other than from the SRTM3 C-Band data with 90 m horizontal resolution was available. The DEM has only few artifacts mainly near the highest Peak Pik Talgar at 4978 m asl. All holes were interpolated using a spline algorithm. For evaluation reasons parts of the final SRTM3 DEM were compared with a DEM derived from Russian topographic maps (1:100,000) from the late 1970s

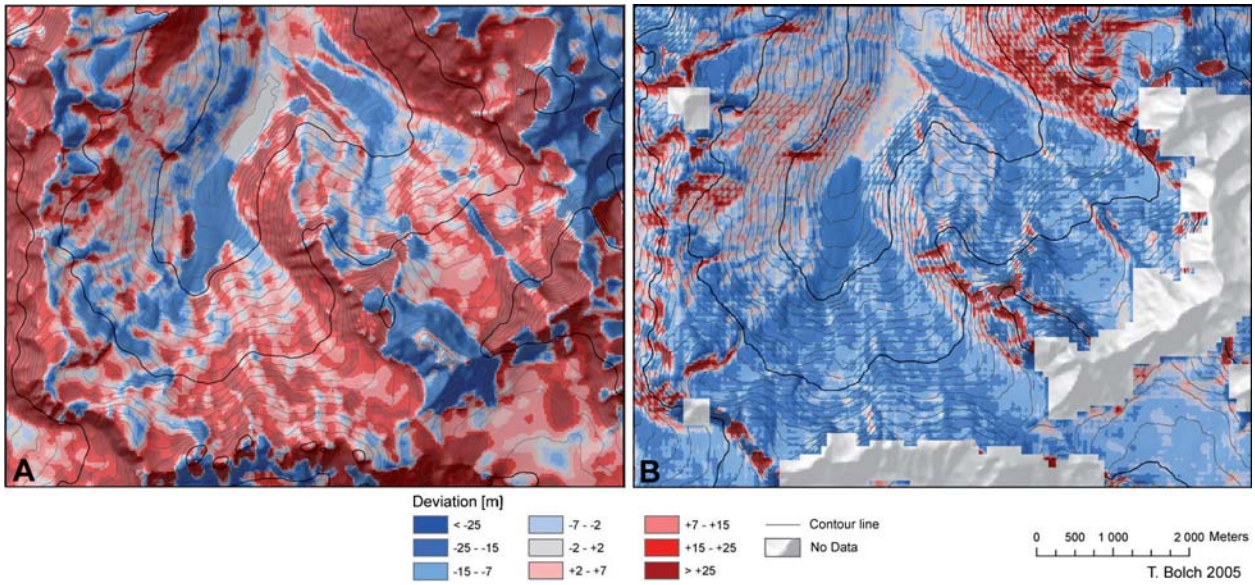

Figure 2: Deviation in elevation of both (A) ASTER DEM and (B) SRTM3 DEM from the reference DHM25L2 for the Bernina Group, Swiss Alps; DHM25 reproduced with the permission of swisstopo (BA057533).

	Min.	Max.	Mean	Std. Dev.	$RSME_z$
ASTER	-269 m	330 m	8.3 m	43.7 m	28.4 m
SRTM3	-192 m	210 m	-9.8 m	17.1 m	9.8 m

Table 1: Deviation in elevation of both ASTER DEM and SRTM3 DEM from the reference DHM25L2 for the Bernina Group, Swiss Alps.

with an equidistance of 40 m. For the latter a spline-with-tension algorithm was used for interpolation. Both DEMs match very well, especially in areas of smooth slope angles, whereas larger differences occur in steeper terrain (Figure 3). In general, SRTM DEM elevations are slightly lower, whereas the DEM derived from the Russian maps offers some more topographical detail (Table 2). With +283 m and -297 m the maximum and minimum deviations are high. The reason for this is the replacement of steep slopes by hachures in the contour DEM, i.e. accurate digitizing was somewhat problematic. Certainly the SRTM3 DEM is usable for glacier mapping.

A third DEM was generated from two ASTER Level 1A scenes: one from October 2000 (cloud cover 5%) covering the northern part of the study area; another from September 2001 (cloud cover 20%) covering the southern part. All in all 33 GCPs from fieldwork and topographic maps (1:100,000) and 45 TPs were collected. The total RMSEx,y was <20 m for the GCPs and <8 m for the TPs. Artifacts in the raw DEM mainly resulted from clouds. Thus, cloud-covered areas were therefore marked, clipped and filled with SRTM3 data. A seamless transition between the two data sets was achieved using a blending tool of the SAGA software. Since the overall quality of the final ASTER DEM is good, there was no need for further post-processing (Bolch et al., 2005).

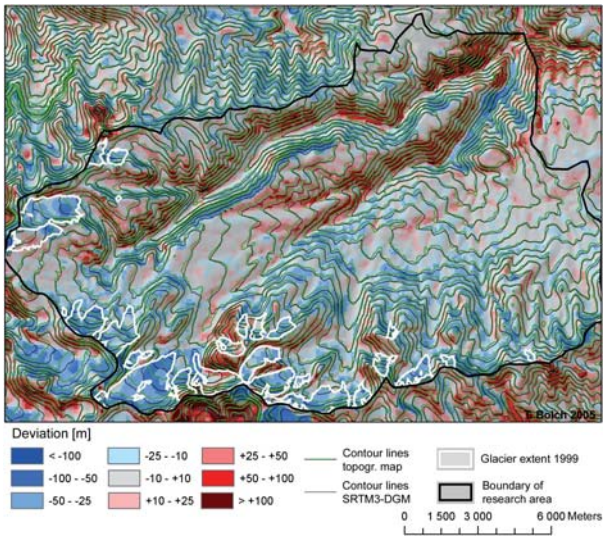

Figure 3: Deviation in elevation of the SRTM3 DEM from the DEM from contour lines for the Tien Shan study area.

Min.	Max.	Mean	Std. Dev.	$RSME_{X,Y}$
-297 m	+283 m	-1.9 m	39.3 m	28.3 m

Table 2: Deviation in elevation of the SRTM3 DEM from the DEM from contour lines for the Tien Shan study area.

5. Glacier Mapping from Multispectral Images

5.1. Bernina Group, Swiss Alps

Ratio images have been successfully used for the delineation of glaciers for the Swiss Glacier Inventory (SGI) and a study in the Inner Tien Shan (Narama et al., 2006; Paul et al., 2002). In this study, a Landsat ETM+ scene from Sep-

tember 13, 1999 covering the Bernina Group in the Swiss Alps was downloaded for free from the Global Landcover Facility (GLF) at the University of Maryland. Although the main glacier tongues are snow-free, few clouds partly cover upper parts of some glaciers mainly at southern slopes. In a first step, TM4/TM5- and TM3/TM5-ratio images were calculated and segmented using a threshold value of 1 (Figure 4). In the TM3/TM5-ratio image nearly all debris-free ice areas could be identified. At the same time, several shaded slopes were over-emphasised, and all water bodies were misclassified as glaciers. Overall, the TM4/TM5-ratio image resulted in a better classification.

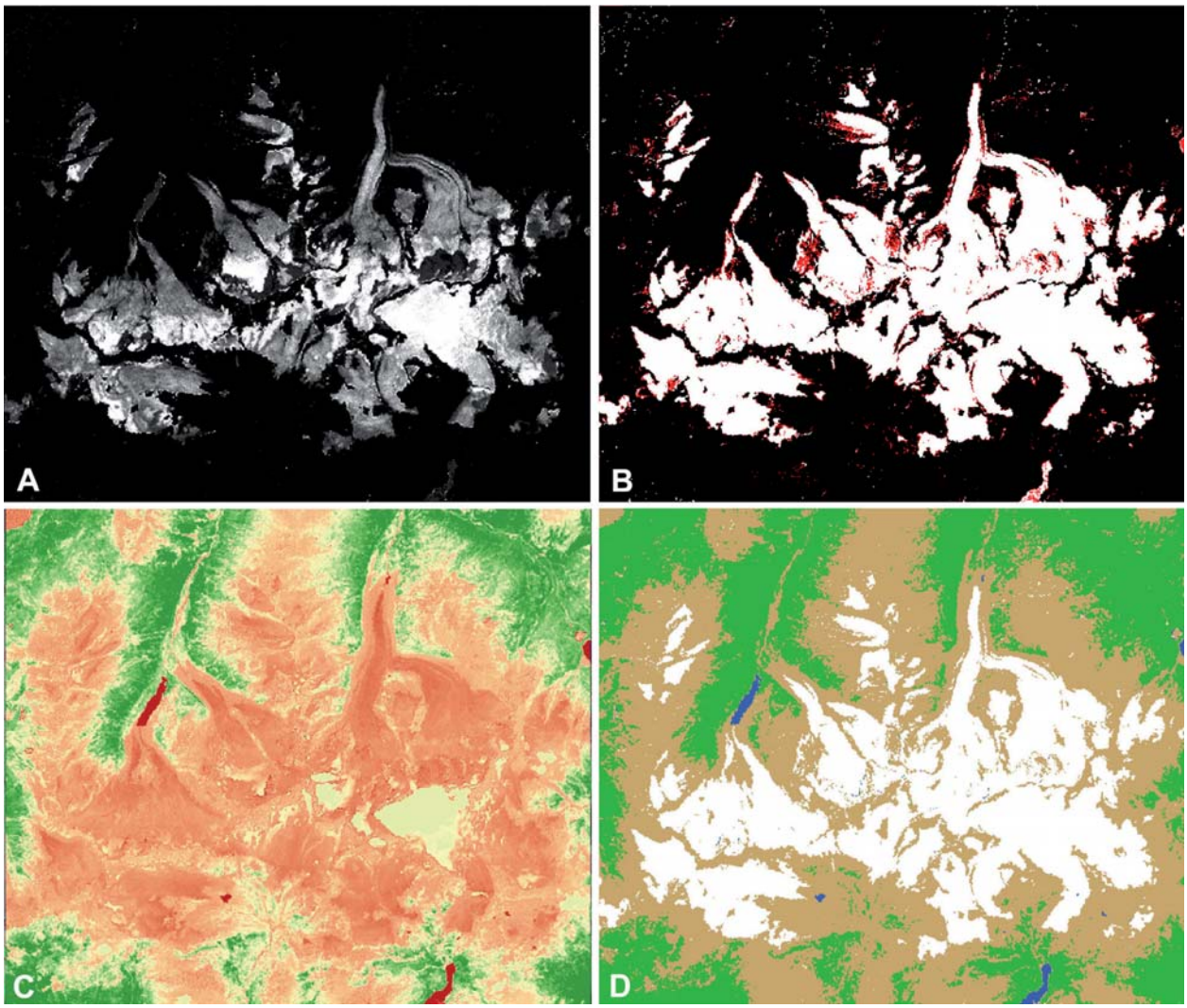

Figure 4: Bernina Group, Swiss Alps. (A) TM4/TM5-ratio image; (B) delineation TM4/TM5 >1 (white), delineation TM3/TM5 >1 (white and red); (C) NDVI; (D) delineation of glaciers (white), vegetated areas (green), water (blue), rock and debris (brown).

In a second step, three land cover classes could be identified using the Normalized Difference Vegetation Index (NDVI): water bodies (NDVI <-0.4), non-vegetated areas (-0.4–0.01), and vegetated areas (NDVI >0.01). As a result nearly all former misclassified pixels in vegetated areas and water bodies were eliminated. However, single pixels in shaded areas (<1% of entire area) still remained misinterpreted as glacier ice. Those pixels were first converted to vector data, then identified by size setting the threshold to 200 m², and finally deleted. Still problematic remained debris-covered and cloud-covered areas as well as areas in dark shadow (Figure 5). One way to eliminate these failures could be manual delineation, but unfortunately, even such visual interpretation is difficult in debris-covered areas and areas in dark shadow. For areas under clouds only a DEM and/or field experience supports the mapping.

In the evaluation of the glacier delineation the 1999 glacier polygons of the Swiss Glacier Inventory (SGI, Paul 2003) were used. By employing only the ratio images the glaciated areas are approximately 5% to small, whereas an

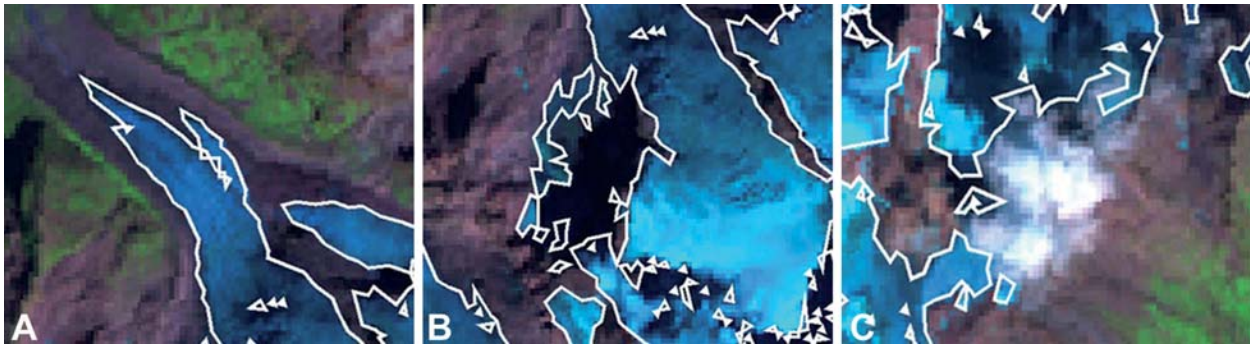

Figure 5: Problematic areas for delineation of glaciers in the Bernina Group, Swiss Alps. (A) debris cover; (B) dark shadow; (C) clouds.

(1) TM4/TM5-ratio image	(2) Ratio image plus manual mapping	(3) Glaciated area from SGI	Difference (2) to (1)	Difference (3) to (2)
60,80 km²	64,13 km²	64,62 km²	-5,2%	-0,8%

Table 3: Results for delineation of glaciers in the Bernina Group, Swiss Alps, following different approaches.

additional manual mapping leads to very similar results to the Swiss Glacier Inventory (Table 3). The remaining only small variation of <1% originates in the experts' interpretations of the debris-covered areas and the small cloud.

and in some debris-covered glacier parts (Fig. 6). An evaluation of results was carried out for the Malaya-Almatinka Valley, for which a detailed topographic map 1:10,000 based on a 1998 field campaign exists (Eder et al., 2002).

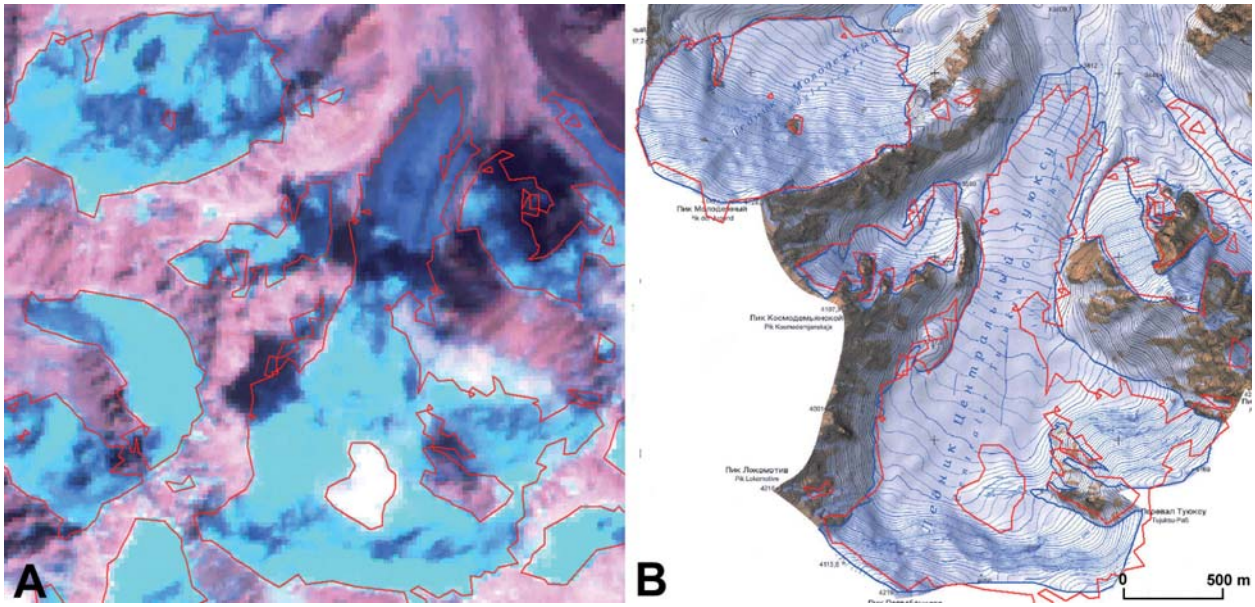

Figure 6: Northern Tien Shan. (A) Delineated glaciated areas in Malaya-Almatinka-Valley using TM4/TM5-ratio images; (B) comparison with glacier outlines in the topographic map 1:10,000 (Eder et al., 2002).

5.2. Northern Tien Shan, Kazakhstan and Kyrgyzstan

The same mapping approach was also applied to glaciers in the northern Tien Shan. Landsat ETM+ imagery from August 8, 1999 was downloaded for free from GLF. The glacier tongues are snow-free, but a few clouds partly cover some glaciers mainly at southern slopes. Again, the mapping results from the TM4/TM5-ratio image are of high accuracy, and this is even true for shaded snow and ice surfaces. Problems still appear in areas under clouds

Again, glacier parts under cloud cover required a manual elimination. Differences between the corrected areas in the imagery and the corresponding areas in the topographic maps are only around 3% (Table 4).

6. Morphometric Glacier Mapping

6.1. Bernina Group, Swiss Alps

A morphometric glacier mapping (MGM) of debris-covered glaciers in the Bernina Group followed the approach

Glacier	Area 1998 (TopoMap 1:10000) [km²]	Area 1999 (Landsat, original) [km²]	Area 1999 (Landsat, improved) [km²]	Area 1999 (WGMS) [km²]	Difference in Area Landsat improved to TopoMap [%]
Molodezhnyj	1.16	1.12	1.12	n. a.	-0.04 (-3.4%)
Zon Kosmodemjan	0.24	0.22	0.22	n. a.	-0.02 (-8.3%)
Tsentralnyj Tuyuksu	2.60	2.19	2.51	2.56	-0.09 (-3.5%)
Igli Tuyuksu	1.21	1.12	1.19	n. a.	-0.02 (-1.7%)
Ordzhonikidze	0.25	0.24	0.24	n. a.	-0.01 (-4.0%)
Mayakovskogo	0.12	0.11	0.11	n. a.	-0.01 (-8.3%)
Manshik Mametovoj	0.32	0.33	0.33	n. a.	+0.01 (+3.0%)
Total	**5.90**	**5.33**	**5.72**	**n. a.**	**-0.18 (-3.1%)**

Table 4: Northern Tien Shan. Glaciated areas in the Malaya-Almatinka Valley delineated from the topographic map 1:10,000 after Eder et al. (2002), from Landsat imagery, and from the World Glacier Monitoring Service (WGMS).

presented by Paul et al. (2004). First, slope angles were calculated using the DHM25L2 and setting the threshold to 24°, which helps to identify smoother glacier parts, in particular in the ablation zone. Problematic is the determination of the boundary between glacier terminus and outwash plain (Figure 7a). Furthermore, glaciers without any lateral moraines are difficult to delineate. Although a lower threshold of 18° improves the delineation of the terminus, several "glacier pixels" are now excluded. Last but not least, several glaciers with a more complex morphology show some classification inhomogeneity due to existing icefalls or steeper terminus slopes. Paul et al. (2004) experienced similar problems and suggested a multitemporal approach. The glaciers were also mapped using the SRTM3 DEM. Using only the slope for the morphometric analysis led to misinterpretations of the glacier terminus and the lateral moraines, since here resolution and precision of the SRTM3 DEM are insufficient (Figure 7b). Using the ASTER DEM did not lead to significantly better results. Nevertheless, for the Grosser Aletschgletscher in the Swiss Alps Paul et al. (2004) found ASTER DEMs of good use for glacier delineation, although accepting higher inaccuracies than using the DHM25L2.

In the DHM25L2, which represents the glacier extent of the year 1991, the shaded relief allows for identification of glacier tongues and lateral moraines of Tschierva Glacier (Figure 8a). Since the MGM using the slope alone did not lead to satisfying results, the DHM25L2 had first to be smoothed with a 3x3 filter to obtain more homogenous areas. Following the approach of Schmidt and Dikau (1999) for describing landforms, plan curvature and profile curvature were now employed for glacier mapping, and both were calculated after Zevenberg and Thorne (1987) using the software SAGA. A cluster analysis combined surfaces of similar characteristics. An aggregation of ten clusters showed best results (Figure 8b). In particular, glacier surfaces and valley bottoms and other areas of no or poor convexity represented by the light bluish-grayish color are recognizable. Dark blue and green colors represent (strongly) convex areas such as ridges and lateral mo-

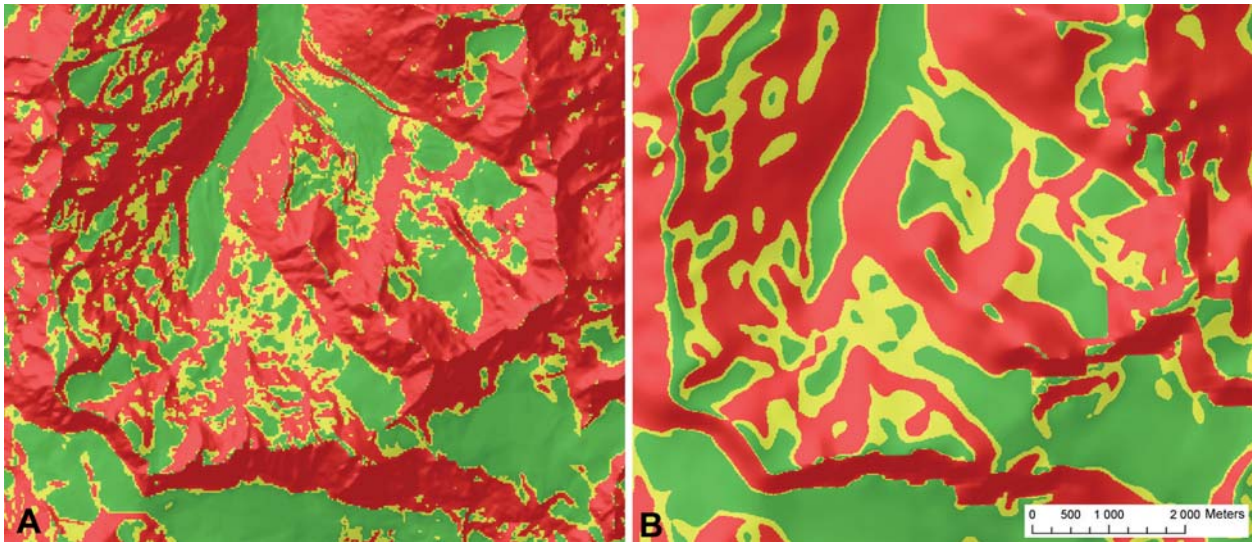

Figure 7: Classification of slope at Tschierva Glacier and Roseg Glacier, Bernina Group, Swiss Alps. Green: <18°; yellow: 18 – 24°; red >24°. (A) DHM25L2; (B) merged SRTM3/ASTER-DEM ; DHM25 reproduced with the permission of swisstopo (BA057533).

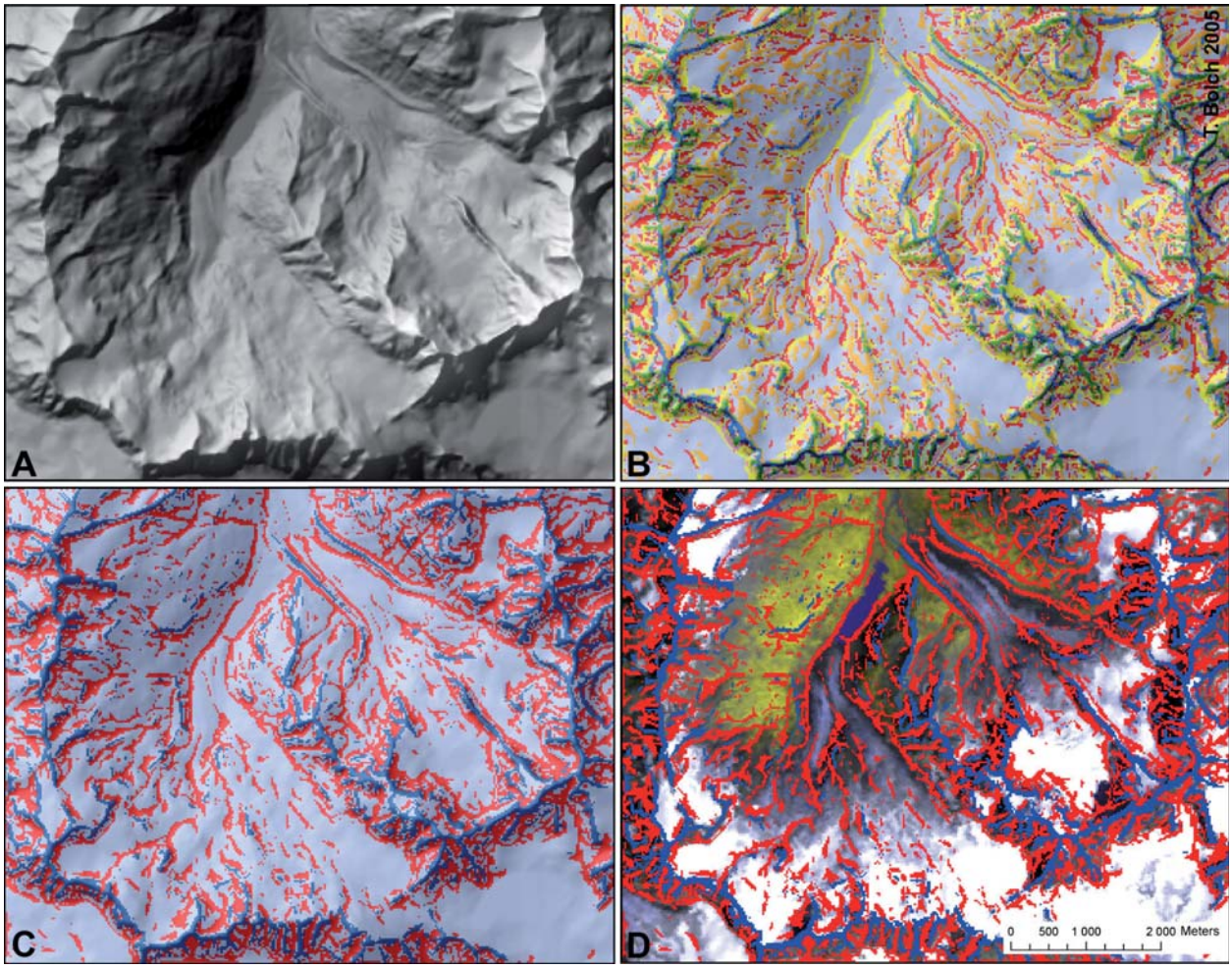

Figure 8: Morphometric glacier mapping of Roseg Glacier and Tschierva Glacier. (A) Shaded DHM25L2; (B) clusters of plan and profile curvature; (C) reduction to three clusters; (D) clusters overlying Landsat scene from 1992 ; DHM25 reproduced with the permission of swisstopo (BA057533).

raines. Orange color represents moderate convexity which can be found, for instance, at medial moraines. Red and yellow colors are (strongly) concave parts such as transitions between glacier margins and lateral moraines. In a next step the number of clusters was reduced to three by taking account of the described curvature characteristics (Figure 8c). The final result is an improved glacier delineation which includes debris-covered glacier parts (Figure 8d). The described MGM method also helps to map the accumulation zone of glaciers and smaller mountain glaciers, although some inaccuracies still exist. However, both are often free from debris-cover, therefore here the ratio image method is the better choice for mapping.

The MGM method was also tested using the SRTM3 DEM, which resolution and accuracy are lower than for the DHM25L2 and which represents the glacier extent of early 2000 (Figure 9a). In general, delineation results are of lower quality, although the main curvature classes are properly represented and glacier tongues can still be identified (Figure 9b-d). For the study area, employing the ASTER DEM for such analysis does not improve the mapping results.

6.2. Northern Tien Shan, Kazakhstan and Kyrgyzstan

For the Tien Shan, the MGM method was applied to glaciers in the Malaya-Almatinka Valley. In general, supraglacial debris covers relatively small areas (<3%), and mainly the glacier terminus of the largest valley glacier Tsentralniy Tuyuksu. The SRTM3-DEM first was resampled to a 30 m horizontal resolution, and then plan and profile curvature were extracted and classified into ten clusters. Landform elements are well defined; dark blue colors represent high convexity of mountain ridges, and light blue color represents areas of very low convexity such as glaciers and valley bottoms (Figure 10a). Larger glaciers are well identifiable such as in the Chilik Valley where glaciers have relatively dense debris-covers. Using only the TM4/

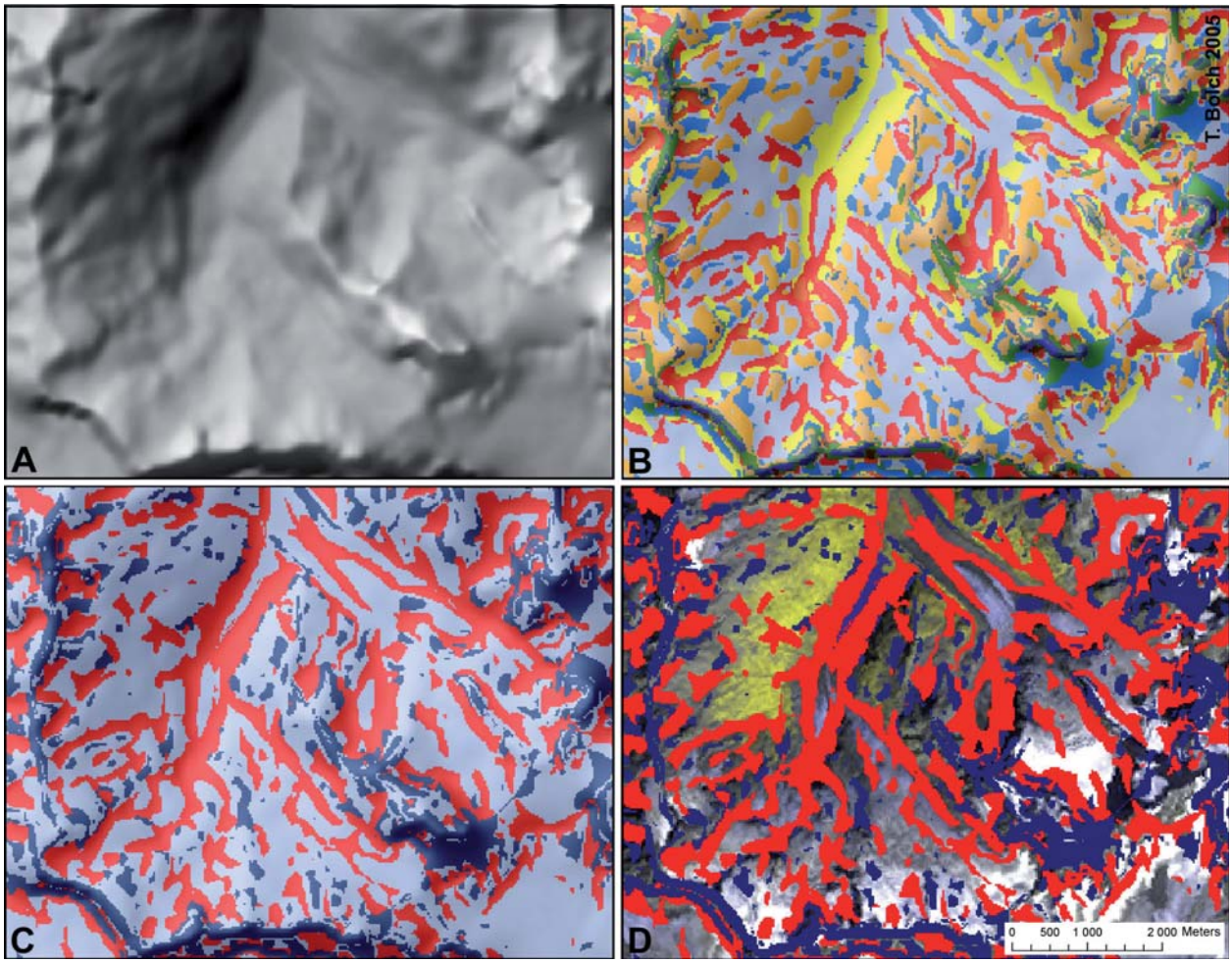

Figure 9: Morphometric glacier mapping of Roseg Glacier and Tschierva Glacier. (A) Shaded SRTM3 DEM; (B) clusters of plan and profile curvature; (C) reduction to three clusters; (D) clusters overlying Landsat scene from 1999.

TM5-ratio image for the delineation of the Novyj Glacier leads to insufficient results (Figure 10b). However, the MGM approach correctly identifies the entire terminus (Figure 10c). Again, this proves the capability of the MGM method for valley glacier mapping. Employing the ASTER DEM did not significantly improve the results.

7. Conclusion

For the Bernina Group in the Central Alps the comparison between the Swiss DHM25L2, the SRTM3 DEM and a generated ASTER DEM revealed elevation inaccuracies of the two latter ones. Whereas ASTER DEM elevations are often too high, SRTM3 DEM elevations are often slightly too low. Due to a higher horizontal resolution, smaller landforms are identifiable in the raw ASTER DEM. However, post-processing procedures for eliminating holes, peaks, pits and stripes cause loss of accuracy and detail. This was especially true for the Bernina Group, where in the end the ASTER DEM was not more useful than the SRTM3 DEM of lower horizontal resolution. Nevertheless, for the Grosser Aletschgletscher in the Swiss Alps Paul et al. (2004) found ASTER DEMs of good use for glacier delineation. On the other hand, for the Swiss study area the SRTM3 DEM lacks data points at mountain peaks and steep slopes due to the radar shadow effect. However, such areas can be substituted by ASTER DEM data (see also Kääb, 2005). The main advantage of ASTER DEMs is the capability to generate multitemporal DEMs which supports glacier monitoring studies.

Following the approach of Paul et al. (2002), a glacier mapping using a TM4/TM5-ratio image in combination with a multispectral image analysis to eliminate misclassified pixels was successfully applied to clean-ice glaciers in both study areas. Bolch (2006) followed this method to map glacier changes in the northern Tien Shan. For debris-covered glaciers or glacier parts, an additional morphometric glacier mapping approach (MGM) that focuses on curvature characteristics is capable to identify also supraglacial debris. However, results heavily depend on resolution and quality of the employed DEM as well as the

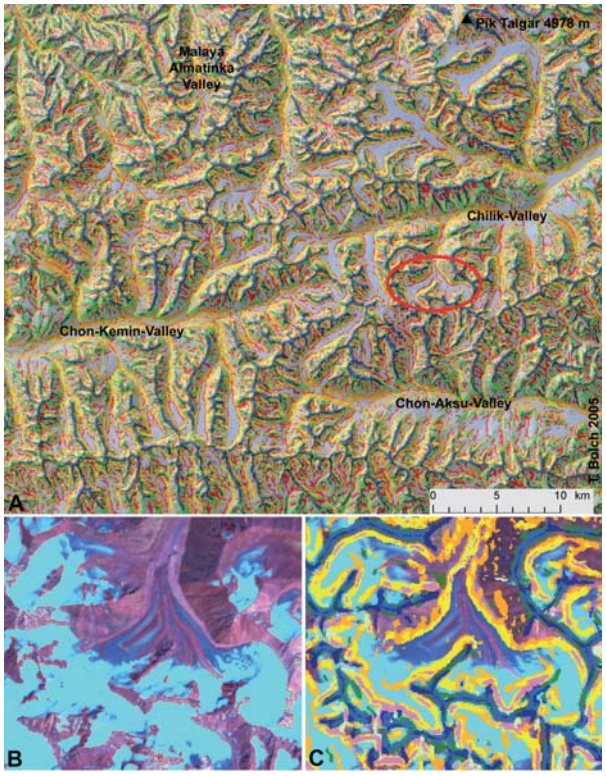

Figure 10: SRTM3 DEM of the Northern Tien Shan. (A) Cluster of plan and profile curvature; red circle: Novyj Glacier; (B) ratio image of debris-covered Novyj Glacier in Chilik Valley; (C) same glacier delineated using the MGM approach resulting in three curvature clusters.

specific glacier characteristics such as surface features. Larger valley glaciers in the Bernina Group were successfully identified using the DHM25L2. Using the ASTER DEM or the SRTM3 DEM the delineation resulted in higher inaccuracies. For the northern Tien Shan, where no detailed DEM exists, the MGM approach in combination with ASTER DEMs or SRTM3 DEMs led to good delineation results for larger valley glaciers.

Ongoing studies focus on an automation of the MGM approach for debris-covered glaciers.

8. Acknowledgements

The authors would like to thank Manfred Buchroithner (Technical University Dresden, Germany) for helpful discussions and comments, and Frank Paul (University Zurich, Switzerland) for providing the glacier polygons of the Swiss Glacier Inventory. ASTER data was provided at no cost by NASA/USGS. SAGA software is available at: http://www.saga-gis.uni-goettingen.de/html/index.php.

This is a base study for the project "Monitoring of glaciers and glacial lakes at Mt. Everest, Nepal using ASTER data and digital elevation models" funded by the German Research Foundation (DFG) under the title BU 949/15-1.

References

BAYR, K. J., HALL, D. K. and KOVALICK, W. M., 1994: Observations on glaciers in the eastern Austrian Alps using satellite data. International Journal of Remote Sensing 15, 1733-1742.

BISHOP, M. P., KARGEL, J. S., KIEFFER, H., MACHINNIN, D. J., RAUP, B. and SHRODER, J. F., 2000: Remote sensing science and technology for studying glacier processes in high Asia. Annals of Glaciology 31, 164-170.

BISHOP, M. P., BONK, R., KAMP, U. and SHRODER, J.F., 2001: Terrain analysis and data modeling for alpine glacier mapping. Polar Geography 25, 182-201.

BOLCH, T., 2006: Climate change and glacier retreat in northern Tien Shan (Kazakhstan/Kyrgyzstan) using remote sensing data. Global and Planetary Change, in press.

BOLCH, T. and KAMP, U., 2003: Qualitätsanalyse digitaler ASTER-Geländemodelle von Hochgebirgsregionen (Cerro Sillajhuay, Chile/Bolivien). Kartographische Nachrichten 5, 224-230. (In German).

BOLCH, T., KAMP, U. and OLSENHOLLER, J., 2005: Using ASTER and SRTM DEMs for studying geomorphology and glaciation in high mountain areas. New Strategies for European Remote Sensing. M. Oluic (Ed.) Millpress, Rotterdam, 119-127.

BÜYÜKSALIH, G., KOCAK, G. and JACOBSEN, K. 2004: Quality assessment of DEM derived from the SRTM X- and C-band Data: A Case Study for Rolling Topography and Dense Forest Cover. Proceedings of the EARSeL Workshop "Remote Sensing for Developing Countries" held in Cairo 2004, 6p. accessed online January 2005: http://www.ipi.uni-hannover.de/html/publikationen/2004/paper/Büyük_etal_Cairo04.pdf

DELLA VENTURA, A., RAMPINI, A., RABAGLIATI, R. and BARBERO, R. S., 1987: Development of a satellite remote sensing technique for the study of alpine glaciers. International Journal of Remote Sensing 8, 203-215.

DIKAU, R., BRABB, E. E., MARK, R. K. and PIKE, R. J., 1995: Morphometric landform analysis of New Mexico. Zeitschrift fur Geomorphologie, Suppl.-Bd. 10, 109-126.

ECKERT, S., KELLENBERGER, T. and ITTEN, K., 2005: Accuracy assessment of automatically derived digital elevation models from ASTER data in moun-

tainous terrain. International Journal of Remote Sensing 26, 1943-1957.

EDER, K., GEISS, T. and HORNIK, H., 2002: Neukartierung und DGM-Aufbau für das Tujuksu-Gletschergebiet im Tian Shan. Zeitschrift für Gletscherkunde und Glazialgeologie 38, 129-138. (In German).

GRATTON, D. J., HOWARTH, P. J. and MARCEAU, D. J., 1990: Combining DEM parameters with Landsat MSS and TM imagery in a GIS for mountain glacier characterization. IEEE Transactions on Geoscience and Remote Sensing 28, 766-769.

GSPURNING, J. and SULZER, W., 2004: DEM-Generierung aus ASTER-Daten und Evaluierung. In: STROBL, J., T. BLASCHKE UND G. GRIESEBNER (Hg.). 2004. Angewandte Geoinformatik 2004 - Beiträge zum 16. AGIT-Symposium Salzburg. Heidelberg, 190-195.

HEMPEL, A., 2005: Vergleich von Methoden zur Abgrenzung schuttbedeckter Gletscher im Khumbu Himal mit ASTER- und Landsatdaten. Semester Thesis, Department of Cartography, Technical University Dresden, 70 pp. (In German).

JACOBSEN, K., 2005: Analysis of digital elevation models based on space information. New Strategies for European Remote Sensing. In: M. OLUIC (Ed.), Millpress, Rotterdam, 439-451.

KÄÄB, A., 2005: Combination of SRTM3 and repeat ASTER data for deriving alpine glacier flow velocities in the Bhutan Himalaya. Remote Sensing of Environment 94/4, 463-474.

KÄÄB, A., HUGGEL, C., PAUL, F., WESSELS, R., RAUP, B., KIEFFER, H., KARGEL, J. S., 2003: Glacier monitoring from ASTER imagery. Accuracy and applications. EARSeL eProceedings 2 - Observing our cryosphere from space, 43-53.

KAMP, U., BOLCH, T. and OLSENHOLLER, J., 2005: Geomorphometry of Cerro Sillajhuay, Chile/Bolivia: comparison of DEMs derived from ASTER remote sensing data and contour maps. Geocarto International 20, 23-34.

NARAMA, C., SHIMAURA, Y., NAKAYAMA, D. and ABDRAKHMATOV, K. E. 2006: Recent changes of glacier coverage in the western Terskey-Alatoo Range, Kyrgyz Republic, using Corona and Landsat. Annals of Glaciology, in press.

OERLEMANS, J., 1994: Quantifying global warming from the retreat of glaciers. Science 264, 243-245.

PAUL, F., 2000: Evaluation of different methods for glacier mapping using Landsat TM. EARSeL eProceedings 1 - Land Ice and Snow, 239-245.

PAUL, F., 2002: Changes in glacier area in Tyrol, Austria, between 1969 and 1992 derived from Landsat 5 TM and Austrian Glacier Inventory data. International Journal of Remote Sensing 23, 787-799.

PAUL, F., 2003: The New Swiss Glacier Inventory 2000: Application of Remote Sensing and GIS. Ph.D. Thesis, Department of Geography, University Zurich, 154 .

PAUL, F., KÄÄB, A., MAISCH, M., KELLENBERGER, T., HAEBERLI, W., 2002: The new remote sensing derived Swiss Glacier Inventory: I. Methods. Annals of Glaciology 34, 355-361.

PAUL, F., HUGGEL, C., KÄÄB, A. and KELLENBERGER, T., 2003: Comparison of TM-Derived Glacier Areas with Higher Resolution Data Sets. EARSeL eProceedings 2 - Observing our cryosphere from space, 15-21.

PAUL, F., HUGGEL, C. and KÄÄB, A. 2004: Combining satellite multispectral image data and a digital elevation model for mapping of debris-covered glaciers. Remote Sensing of Environment 89, 510-518.

RANZI, R., GROSSI, G., IACOVELLI, L. and TASCHNER, T., 2004: Use of multispectral ASTER images for mapping debris-covered glaciers within the GLIMS Project. IEEE International Geoscience and Remote Sensing Symposium 2, 1144-1147.

SCHMIDT, J. and DIKAU, R., 1999: Extracting geomorphometric attributes and objects from digital elevation models - semantics, methods, future needs. In: R. DIKAU and H. SAURER (Ed.): GIS for Earth Surface Systems: Analysis and Modeling of the Natural Environment, Berlin, 153-173.

SIDJAK, R. W. and WHEATE, R. D., 1999: Glacier mapping of the Illecillewaet icefield, British Columbia, Canada, using Landsat TM and digital elevation data. International Journal of Remote Sensing 20, 273-284.

Swisstopo, 2004: DHM25 - Das digitale Höhenmodell der Schweiz. Bundesamt für Landestopographie, 15 p., www.swisstopo.ch

WILLIAMS, R. S., HALL, D. K., SIGURDSSON, O. and CHIEN, J. Y. L., 1997: Comparison of satellite-derived with ground-based measurements of the fluctuations of the margins of Vatnajökull, Iceland, 1973-1992. Annals of Glaciology 24, 72-80.

ZEVENBERG, L. W. and THORNE, C. R., 1987: Quantitative analysis of land surface topography. Earth Surface Processes and Landforms 12, 47-56.

Correspondance to:

TOBIAS BOLCH

Institute for Cartography

Dresden University of Technology

Helmholtzstraße 10

D-01062 Dresden, Germany

Tel.: +49 351 463-35495

Fax: +49 351 463-37028

E-mail: tobias.bolch@tu-dresden.de